PROCEEDINGS OF THE ROYAL SOCIETY A MATHEMATICAL, PHYSICAL & ENGINEERING SCIENCES

Review of statistical energy analysis hypotheses in vibroacoustics

T. Lafont, N. Totaro and A. Le Bot

Proc. R. Soc. A 2014 **470**, 20130515, published 4 December 2013

PROCEEDINGS OF THE ROYAL SOCIETY A

rspa.royalsocietypublishing.org

Review of statistical energy analysis hypotheses in vibroacoustics

T. Lafont[1,2], N. Totaro[2] and A. Le Bot[1]

[1]Laboratoire de Tribologie et Dynamique des Systemes, Ecole Centrale de Lyon, 36 Avenue Guy de Collongues, 69134 Ecully Cedex, France

[2]Laboratoire Vibrations Acoustique, INSA-Lyon, Batiment St Exupery, 25 bis Avenue Jean Capelle, 69621 Villeurbanne Cedex, France

Research

Cite this article: Lafont T, Totaro N, Le Bot A. 2014 Review of statistical energy analysis hypotheses in vibroacoustics. *Proc. R. Soc. A* **470**: 20130515.
http://dx.doi.org/10.1098/rspa.2013.0515

Received: 2 August 2013
Accepted: 5 November 2013

Subject Areas:
acoustics, wave motion, structural engineering

Keywords:
statistical energy analysis, diffuse field, energy equipartition, rain-on-the-roof excitation

Author for correspondence:
T. Lafont
e-mail: thibault.lafont@cpe.fr

This paper is a discussion of the equivalence between rain-on-the-roof excitation, diffuse field and modal energy equipartition hypotheses when using statistical energy analysis (SEA). A first example of a simply supported plate is taken to quantify whether a field is diffuse or the energy is equally distributed among modes. It is shown that the field can be diffuse in a certain region of the frequency-damping domain with a single point force but without energy equipartition. For a rain-on-the-roof excitation, the energy becomes equally distributed, and the diffuse field is enforced in all regions. A second example of two plates coupled by a light spring is discussed. It is shown that in addition to previous conclusions, the power exchanged between plates agrees with the statistical prediction of SEA if and only if the field is diffuse. The special case of energy equipartition confirms this observation.

1. Introduction

The statistical energy analysis (SEA) is a method introduced by Lyon and co-workers [1–3] in the 1960s intended to estimate the vibroacoustic response of complex structures in the high-frequency range by a statistical approach. This is the analogous of statistical mechanics for structural dynamics and as such could be called statistical vibroacoustics [4]. However, the difficulties encountered when using SEA for engineering purposes have motivated many studies on the required assumptions and have divided the opinions of the scientific community on their status.

Royal Society Publishing

The main result of SEA is the so-called 'coupling power proportionality'. It states that the mean power exchanged between two subsystems is proportional to the difference of modal energies [5]. The modal energy thus plays the role of vibrational temperature, and the 'convective coefficient' is called coupling loss factor. Regarding the foundations, there are several manners to approach SEA: the modal and the wave approaches. Fahy [6] gives a retrospective for each one. The modal approach of SEA starts from the basic equations of mechanical oscillators excited by random forces and proves the existence of the coupling loss factors [1,2,7], whereas the wave approach is based on the evaluation of the reflection and transmission coefficients at a junction [8–10] (considering plane waves) and provides effective relationships for the coupling loss factors. Using these concepts, the question of the equivalence between the hypotheses used in both approaches is raised.

This work is a discussion on the assumptions of energy equipartition, rain-on-the-roof and diffuse field. Although a complete derivation of SEA requires some other assumptions that would also merit discussion, these three hypotheses are at the core of the wave/modal duality of SEA. Their choice allows the highlighting of the conceptual equivalence of both approaches. One has also chosen to stay in the strict vision of SEA (assuming conservative, weak and direct coupling) for which the mathematical derivations are more rigorous and unquestionable. In this regard, one must mention the numerous extensions of SEA to strong coupling [11], non-conservative coupling [12–14], indirect coupling [15], non-uniform modal energy distribution [16–18], non-uniform directional energy distribution [19] and non-uniform spatial energy distribution [20,21].

In what follows, the two approaches of SEA are reviewed to highlight the usefulness of all assumptions in the derivation of the coupling power proportionality equation. The three hypotheses under discussion are introduced in §3. A benchmark is considered in §4 to evaluate the practical conditions to fulfill these three assumptions. In §5, an example of two coupled subsystems is discussed to verify that the coupling power proportionality holds under previously determined conditions.

2. Basics of statistical energy analysis

The simplest system for which the coupling power proportionality may be stated consists of two mechanical oscillators submitted to uncorrelated random forces as shown in figure 1. The state is described by a unique variable X_i for the position of oscillator i. The governing equations are

$$\left.\begin{aligned} m_1\ddot{X}_1 + M\ddot{X}_2 + c_1\dot{X}_1 + G\dot{X}_2 + k_1X_1 + K(X_1 - X_2) &= F_1 \\ \text{and} \qquad m_2\ddot{X}_2 + M\ddot{X}_1 + c_2\dot{X}_2 - G\dot{X}_1 + k_2X_2 + K(X_2 - X_1) &= F_2, \end{aligned}\right\} \tag{2.1}$$

where m_i are the masses, c_i the viscous damping coefficients and k_i the spring stiffnesses of oscillators. The oscillators are coupled through three constants M, G and K for, respectively, inertial, gyroscopic and elastic couplings. These three kinds of coupling forces ensure that no dissipation occurs in the coupling. With this respect, the first assumption of statistical energy analysis is that *the coupling is conservative*. The external forces F_i are assumed to be random. More exactly, the second assumption of statistical energy analysis is that *the forces are uncorrelated white noises*. In particular, the power spectral densities are constant over the whole frequency band, and the cross power density is null. Under these conditions, it has been proved by Lyon & Maidanik [1] and Scharton & Lyon [22] that the expectation of the power flow between oscillators is proportional to the difference in the expectation of vibrational energies,

$$\langle P_{12}\rangle = \beta(\langle E_1\rangle - \langle E_2\rangle). \tag{2.2}$$

This is the coupling power proportionality. The coefficient β is

$$\beta = \frac{\mu^2(\Delta_1\Omega_2^4 + \Delta_2\Omega_1^4 + \Delta_1\Delta_2(\Delta_1\Omega_2^2 + \Delta_2\Omega_1^2)) + (\gamma^2 + 2\mu\kappa)(\Delta_1\Omega_2^2 + \Delta_2\Omega_1^2) + \kappa^2(\Delta_1 + \Delta_2)}{(1-\mu^2)[(\Omega_1^2 - \Omega_2^2)^2 + (\Delta_1 + \Delta_2)(\Delta_1\Omega_2^2 + \Delta_2\Omega_1^2)]}, \tag{2.3}$$

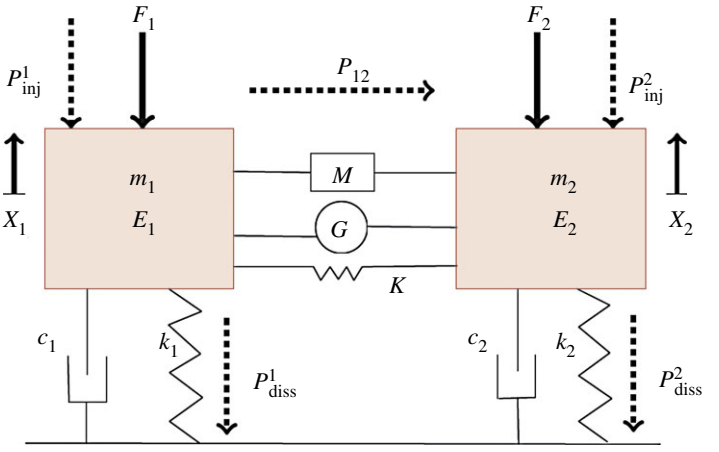

Figure 1. Two oscillators having mass m_i, stiffness k_i and damping c_i excited by uncorrelated random forces F_i are coupled by an inertial M, an elastic K and a gyroscopic G couplings. (Online version in colour.)

where $\Omega_i^2 = (k_i + K)/m_i$, $\Delta_i = c_i/m_i$, $\mu = M/\sqrt{m_1 m_2}$, $\gamma = G/\sqrt{m_1 m_2}$ and $\kappa = K/\sqrt{m_1 m_2}$. Note that in equations (2.2) and (2.3) the system of two oscillators remains deterministic but is excited by random forces. The brackets $\langle\cdot\rangle$ must therefore be interpreted as probability expectation with respect to the stochastic processes F_1 and F_2.

A generalization to an arbitrary number of oscillators is achieved by Newland [23], who introduced the perturbation technique. Defining a small parameter ϵ for the strength of coupling, the asymptotic developments of $\langle P_{ij}\rangle$ and $\langle E_i\rangle$ in powers of ϵ lead to a direct comparison of $\langle P_{ij}\rangle$ and $\langle E_i\rangle - \langle E_j\rangle$. The coupling power proportionality as given in equation (2.2) remains valid up to order two in ϵ for any pair of oscillators with β as in equation (2.3) provided that *the coupling is assumed to be weak* (see [24] for a discussion on weak coupling). This is the third assumption in statistical energy analysis.

The coupling power proportionality also applies to the exchange between groups of oscillators (figure 2) [25–27]. For this purpose, one introduces the notion of subsystem which are groups of oscillators randomly excited by *uncorrelated white noises but with the same level of power spectral density* (rain-on-the-roof excitation).

The usual way to derive the coupling power proportionality in a modal framework is to consider energy equipartition between modes. This is the method followed in [6,25,28–30]. Let us consider two subsystems containing respectively N_1 and N_2 oscillators (henceforth called modes). In each subsystem, the total vibrational energy $\langle E_i\rangle$ (with $i = 1, 2$) is the sum of individual modal energies. Furthermore, the power exchanged $\langle P_{12}\rangle$ is the sum of individual exchanges between any pair of modes (figure 2). By applying the coupling power proportionality to any pair of modes and by assuming *the equipartition of modal energy* (all modes have the same energy $\langle E_i\rangle/N_i$),

$$\langle P_{12}\rangle = B\left(\frac{\langle E_1\rangle}{N_1} - \frac{\langle E_2\rangle}{N_2}\right), \tag{2.4}$$

where factor B is the sum of individual β for all pairs of modes. Assuming in addition that *the number of modes is large* and *the damping is light*, factor B simplifies. For an elastic coupling of stiffness K, factor B reads [13,26,31]

$$B = \frac{\pi K^2 n_2}{2\omega^2 M_1 M_2}, \tag{2.5}$$

where M_i is the total mass of subsystem i and n_2 the modal density of subsystem 2. The conceptual difference between equations (2.3) and (2.5) is that the former requires the exact values of all natural frequencies of all modes, an information computationally costly, in general, which is not

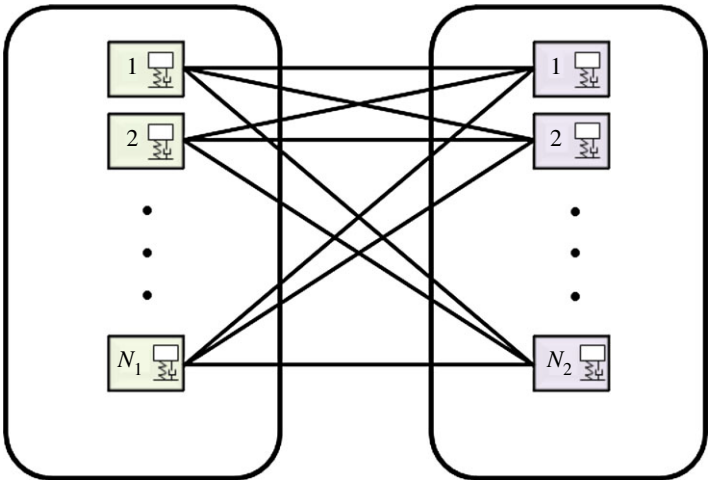

Figure 2. Energy exchanges between two subsystems containing oscillators. (Online version in colour.)

the case for the latter. This justifies the gain in simplicity and consequently in the computation time in using SEA.

In practice, systems are made of structural components which may be beams, plates, shells, acoustical cavities, etc., and the subsystems are generally chosen as these components. In the modal approach to statistical energy analysis, the vibrational field of each component is projected on the modal basis (blocked modes), so that continuous subsystems are reduced to sets of oscillators and consequently all previous conclusions apply and in particular the coupling power proportionality (equation (2.4)) [1,7]. Because the number of modes of continuous structures is infinite, the only further assumption is that the number of modes is truncated. One introduces a frequency bandwidth of analysis in which the power spectral density of excitation is flat. The notion of resonant modes (modes whose natural frequency lies within the frequency band of external excitations) is also introduced. It is assumed that the *only resonant modes contribute to the global response*.

The coupling loss factors are generally difficult to obtain by the modal approach of SEA due to the considerations about distribution of the natural frequencies [32–34]. So, to determine them in all situations of interest, the wave approach of SEA has been introduced [2,3,35]. This second approach of SEA is based on geometrical acoustics [36] and is quite similar to Sabine's theory in room acoustics. The frequency is assumed to be sufficiently high to allow an interpretation in terms of rays, and the energy exchange at an interface is assessed by solving the reflection and transmission coefficients for plane waves. The coupling loss factors are then determined assuming that *the vibrational fields in all subsystems are diffuse*.

Since the early beginning of SEA, application of thermodynamics to structural vibration has been a main concern [37]. But more recently, the thermodynamical approach of SEA aroused a renewed interest, and the coupling power proportionality has been revisited [12,38,39] in particular by application of the second principle of thermodynamics [40,41]. The concept of entropy in SEA may also be interesting [4,42].

In summary, the wave approach of SEA is mainly based on the diffuse field assumption, whereas the modal approach of SEA is based rather on rain-on-the-roof excitation and energy equipartition. These assumptions (figure 3) lead to the same equation of coupling power proportionality (equation (2.4)). This wave/modal duality has been underlined by many authors and has turned out to be a central concept in all subsequent developments in SEA. However, this duality raises many questions such as the equivalence of the three aforementioned required assumptions and their respective domain of validity.

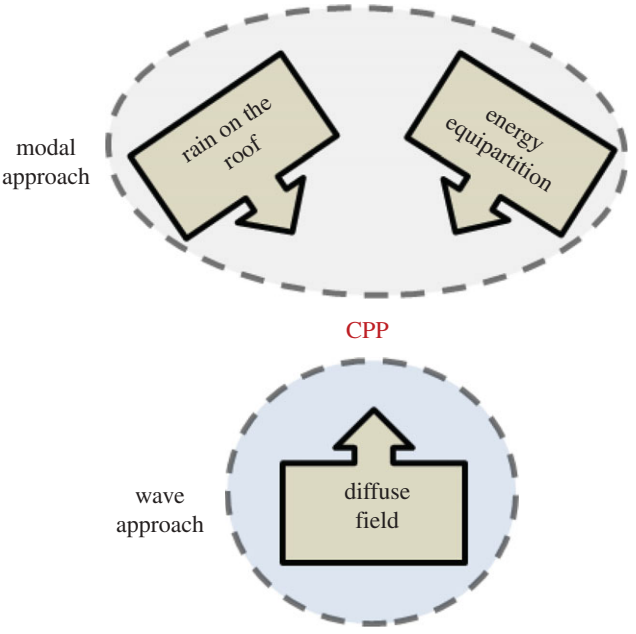

Figure 3. Different ways to obtain the coupling power proportionality—a wave-based approach (diffuse field) and a modal-based approach (energy equipartition or rain on the roof). (Online version in colour.)

The aim of this paper is to examine each hypothesis, to discuss them in some simple examples and evaluate their relevance in regards to the coupling power proportionality.

3. Statistical energy analysis hypotheses

(a) Diffuse field

As discussed by Langley & Shorter [43], two approaches are possible when talking about diffuse field, the wave motion or the resonant modal energy point of view. It leads to different types of definitions. In wave acoustics, Rossi [44] explains that a diffuse field is characterized by a constant sound pressure level during steady state and a linear time decrease spatially independent when sources are switched off. From the geometrical acoustics point of view given by Faller [45], an ideal diffuse sound field is homogeneous and isotropic or, in other words, it is assumed that independent sound waves of equal strength arrive at a receptor (the microphone) from all directions. Lyon [46] proposed a definition of diffuseness from a statistical mechanics point of view where modes are understood as oscillators. When sets of oscillators are taken three conditions must be satisfied: (i) modes are equally energetic within the frequency band, (ii) displacement and momenta of a mode are statistically independent and (iii) the displacements of different modes are statistically independent within the frequency band. Fahy [47] defines diffuse field using the energy density 'the average energy density is the same throughout the volume of the enclosure'. This will be our definition of a diffuse field in this article, the field is considered diffuse if homogeneous. The question of the isotropic nature of a field is not broached here.

(b) Energy equipartition

In statistical physics, equipartition of energy arises under quite general conditions provided that nonlinear interactions between particles ensure the mixing of energy. For instance, in the kinetic

theory of gases, each particle has a random motion and their energy is shared, thanks to their collisions. It should be remembered that equipartition does not mean that all particles (modes in the present context) have the same energy at a fixed time but only that their time-averaged energies are equal [48]. A typical counter-example is that of linear oscillators as this is a non-ergodic system. For such a system, the governing equations projected on the global modal basis are uncoupled, so that the initial repartition of energy among modes remains unchanged in time. However, this does not prevent a spatial reorganization of energy. In particular, an equipartition of energy between coupled oscillators may be observed if the set of natural frequency is fairly disorganized [49]. Magionesi & Carcaterra [50], in their discussion on the validity of the energy equipartition for general engineering systems first recalled the critical aspect related to the applicability formulated in statistical mechanics. Each system of an ensemble has the same structure and the same physical properties 'the hypothesis of a uniform probability of finding representative points of the ensemble of systems over equal-energy-surface in the phase space is assumed', and the assumption of weak coupling is considered. They finally summarized the hypothesis where the energy equipartition principle is supposed to hold: for linear homogeneous and weakly coupled oscillators, energy equipartition may be possible if the same energy quantity is injected via random forces. Calling $\langle E_i^A \rangle$ and $\langle E_k^B \rangle$, the average energies of mode i in subsystem A and mode k in subsystem B; $\langle E^A \rangle$ and $\langle E^B \rangle$ the global energies; N_A and N_B the number of modes, energy equipartition assumption can be written as [29],

$$\langle E_i^A \rangle = \frac{\langle E^A \rangle}{N_A}; \langle E_k^B \rangle = \frac{\langle E^B \rangle}{N_B}. \tag{3.1}$$

(c) Rain-on-the-roof excitation

In the modal approach of SEA, the external force distribution is assumed to be statistically independent [23,28], so that all modes of the structure are excited with the same level. A force field $f(x,t)$ is called rain on the roof if its autocorrelation function is

$$R_{ff}(\chi,\tau) = \langle f(x,t) f(x+\chi, t+\tau) \rangle = \delta(\chi)\delta(\tau) S_0, \tag{3.2}$$

where S_0 is a constant. Let ψ_n the mode shape of mode n, the modal forces $L_n = \int f \psi_n \, \mathrm{d}x$ has the cross-correlation

$$R_{L_n L_m}(\tau) = \langle L_n(t) L_n(t+\tau) \rangle = S_0 \delta(\tau) \delta_{nm} \tag{3.3}$$

by virtue of orthonormality of modes. Thus, for a rain-on-the-roof force field, the corresponding modal forces are uncorrelated white noises with the same power spectral density S_0. The converse is also true.

Fahy [51] pointed out that the special case of point excitation is not valid for SEA in the sense that it does not lead to the same level of modal forces. A strict rain-on-the-roof field corresponds to an infinite number of uncorrelated excitation points. But numerically, such an external force distribution is reduced to a large number of excitation points placed randomly on the structure. In this paper, a quantification is made to evaluate a 'fair' rain-on-the-roof excitation.

4. Benchmark: a single system

A typical issue in SEA is to compute the vibrational response of a structure excited by a random force field. More precisely, one considers a structure excited by either a point force or a set of random point forces having a power spectral density constant in a frequency band. The main goal is to compute the expectation of the local energy $\langle e \rangle(x,y,\omega_c)$ which depends on the receiver point x,y and the frequency band $\Delta\omega$ centred on ω_c. The expectation of modal energy $\langle E_n \rangle(\omega_c)$ depends on the mode index n and the centre angular frequency ω_c. The diffuse nature of a field can be examined by comparing the energy at different points on the structure, whereas the principle of energy equipartition is fulfilled if all modal energies are equal. The rain-on-the-roof hypothesis evaluation is integrated to each of the latter assumptions by increasing the number of excitations when evaluating the diffuse field and energy equipartition criteria.

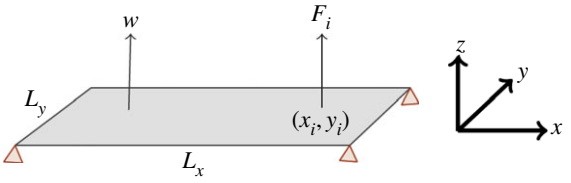

Figure 4. Simply supported plate excited by several random forces having the power spectral density of white noise and the output is the deflection at a receiver point. (Online version in colour.)

(a) Assessment tools of the assumptions

Let us consider a plate having dimensions $L_x \times L_y$ excited by a set of white noise random transverse point forces. The bending rigidity is noted $D = Eh^3/12(1-\nu^2)$, ρ is the mass density, h is the thickness, $m = \rho h$ is the mass per unit area, E is the Young modulus, ν is the Poisson ratio. Figure 4 illustrates the test case.

The equation of motion governing the transverse displacement $w(x, y, t)$ of an undamped plate excited by a force field $f(x, y, t)$ is

$$D\nabla^4 w(x,y,t) + m\frac{\partial^2 w(x,y,t)}{\partial t^2} = f(x,y,t), \tag{4.1}$$

where $\nabla^4 = \partial^4 f/\partial x^4 + \partial^4 f/\partial y^4 + 2(\partial^2/\partial x^2)(\partial^2/\partial y^2)$. In the case of N point sources, the force distribution reads

$$f(x,y,t) = \sum_{i=1}^{N} F_i(t)\delta(x-x_i)\delta(y-y_i), \tag{4.2}$$

where F_i are random functions whose power spectral density $S_i(\omega)$ is assumed constant within the frequency band $\Delta\omega$ and zero elsewhere. Let H be the frequency response function between w at x, y and F_i at x_i, y_i. By a modal decomposition and introducing an *ad hoc* damping loss factor η to account for dissipation, H is given by

$$H(x,y;x_i,y_i;\omega) = \sum_{n\geq 0} \frac{\psi_n(x_i,y_i)\psi_n(x,y)}{m(\omega_n^2 - \omega^2 + j\eta\omega_n\omega)}, \tag{4.3}$$

where ψ_n denotes the mode shape of mode n.

(i) Local energy expectation

The complete expression of the plate energy is given by Soedel [52]. However, for the sake of simplicity, one defines the local energy $e(x, y, t)$ as twice the kinetic energy density. Therefore, the expectation of local energy is

$$\langle e(x,y,t)\rangle = m\langle \dot{w}(x,y,t)^2\rangle. \tag{4.4}$$

The term $\langle \dot{w}^2\rangle$ can be viewed as the autocorrelation function of $\dot{w}$ taken at zero. This is also the Fourier transform of the power spectral density $S_{\dot{w}\dot{w}}$ at zero,

$$\langle \dot{w}(x,y,t)^2\rangle = R_{\dot{w}\dot{w}}(0) = \frac{1}{2\pi}\int_{-\infty}^{+\infty} S_{\dot{w}\dot{w}}(\omega)\,\mathrm{d}\omega. \tag{4.5}$$

But, because forces are uncorrelated, the power spectral density of $\dot{w}$ is related to the power spectral density of forces by,

$$S_{\dot{w}\dot{w}}(\omega) = \sum_{i=1}^{N} \omega^2 |H|^2(\omega) S_i(\omega). \tag{4.6}$$

Combining equations (4.4), (4.5) and (4.6) gives

$$\langle e\rangle(x,y,\omega_c)=\sum_{i=1}^{N}\frac{S_i}{2\pi}m\int_{\Delta\omega}\omega^2|H|^2\,\mathrm{d}\omega, \tag{4.7}$$

where the bounds of the integral have been reduced to $\Delta\omega$, because $S_i(\omega)$ is zero outside. The mean $\langle e\rangle$ does not depend on time for stationary forces. One has added ω_c as variable to highlight the dependance on centre frequency. The problem comes down to the computation of the frequency response function H between any two arbitrary points.

(ii) Modal energy expectation

The global energy can be calculated by integrating the local energy over the plate surface. It yields

$$\langle E\rangle(\omega_c)=\int_0^{L_x}\int_0^{L_y}\langle e\rangle(x,y,\omega_c)\,\mathrm{d}x\,\mathrm{d}y. \tag{4.8}$$

The orthogonality of mode shapes reads $\int_S\psi_n(x,y)\psi_p(x,y)\,\mathrm{d}x\,\mathrm{d}y=\delta_{n,p}$, where $\delta_{n,p}$ is Kronecher's symbol. By combining (4.3), (4.7) and (4.8), the expectation of the global energy is reduced to

$$\langle E\rangle(\omega_c)=\sum_{n\geq 0}\langle E_n\rangle, \tag{4.9}$$

where the modal energy $\langle E_n\rangle$ is

$$\langle E_n\rangle(\omega_c)=\sum_{i=1}^{N}\frac{S_i}{2\pi}\int_{\Delta\omega}\omega^2\frac{\psi_n(x_i,y_i)^2}{m((\omega_n^2-\omega^2)^2+(\eta\omega_n\omega)^2)}\,\mathrm{d}\omega. \tag{4.10}$$

(iii) Diffuse field and energy equipartition criteria

From the distribution of local energy inside a plate, one must estimate whether the field is diffuse or not. To obtain a single criterion, one introduces the standard deviation divided by the mean value of the local energy expectation,

$$\sigma_{\mathrm{d}}=\frac{\sqrt{\overline{\langle e\rangle^2}-\overline{\langle e\rangle}^2}}{\overline{\langle e\rangle}}, \tag{4.11}$$

where the $\overline{(.)}$ operator is defined by $\overline{(.)}=(1/L_xL_y)\iint(.)(x,y)\,\mathrm{d}x\,\mathrm{d}y$.

An analogous approach is adopted with energy equipartition. The criterion is similar to equation (4.11),

$$\sigma_{\mathrm{e}}=\frac{\sqrt{\overline{\langle E_n\rangle^2}-\overline{\langle E_n\rangle}^2}}{\overline{\langle E_n\rangle}}, \tag{4.12}$$

where now $\overline{(.)}=(1/N)\sum_{n=1}^{N}(.)$. When σ_{d} or σ_{e} approaches zero, the local energy is uniformly distributed over the plate or the modal energy is uniformly distributed among modes.

(b) Evaluation and discussion of the three hypotheses

As first example, let us consider a simply supported rectangular plate having characteristics as shown in table 1. The excitations have the same power spectral density constant in an octave band centred on ω_c and their positions are randomly chosen with a uniform distribution. There are 3000 receiver points which are also randomly chosen. Nine octave bands are considered. For a simply supported rectangular plate, the mode index n is a double subscript (α,β), and the expressions of the undamped natural frequencies and the mode shapes are [53] $\omega_n=\sqrt{D/m}((\alpha\pi/L_x)^2+(\beta\pi/L_y)^2)$ and $\psi_n(x,y)=(2/\sqrt{L_xL_y})\sin(\pi\alpha x/L_x)\sin(\pi\beta y/L_y)$. The computation of the local energy follows from equation (4.7) with $S_i=1$ and H given by equation (4.3), where ψ_n and ω_n are as above. However, in the sum of equation (4.3), only resonant modes

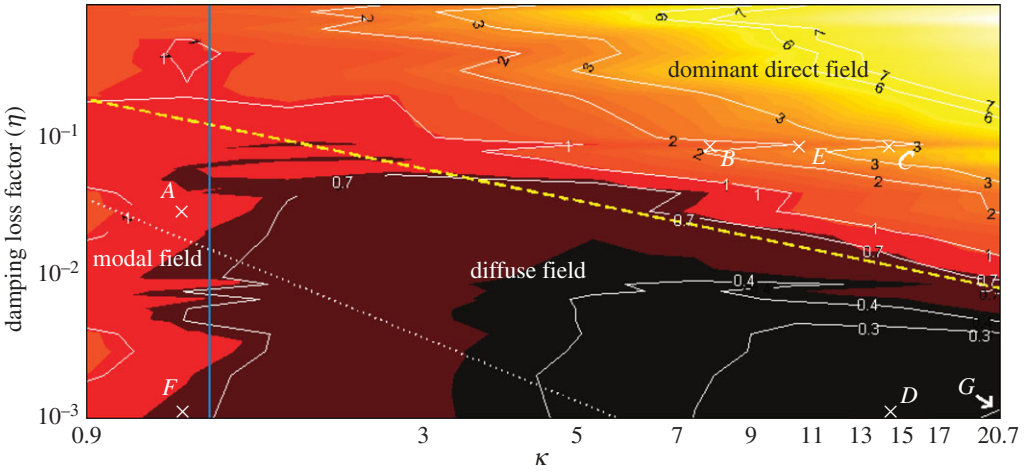

Figure 5. Diffuse field criterion for a rectangular plate excited by a single point force versus wavenumber—damping ratio compared with the modal overlap $M = 1$ (dotted line), the attenuation factor $m = 2$ (dashed line) and the number of modes $N = 10$ (vertical solid line). (Online version in colour.)

Table 1. General parameters of the studied plate.

type	symbol	value	unit
dimensions	$L_x \times L_y$	1.44×1.2	m
density	ρ	7800	kg m^{-3}
Young's modulus	E	2.1E11	N m^{-2}
Poisson's ratio	ν	0.3	—
thickness	h	2	mm
damping coefficient	η	[0.001–0.9]	—
central octave frequency	f_c	[16–8000]	Hz
frequency step	df	$(\eta f_{max})/4$	Hz
mean free path	l	1.0282	m

(modes within the frequency band) have been considered. All non-resonant modes have been simply neglected. The computation of the modal energy and the equipartition criterion follow respectively equations (4.10) and (4.12), again limited to resonant modes.

(i) Diffuse field

Recently, Le Bot & Cotoni [54] proposed validity diagrams on the frequency-damping space to have an idea of how well the SEA method could be applied to a system. It leans on some specific parameters: the number of resonant modes N in the frequency band; the modal overlap M which is defined as the product of the modal density and $\eta\omega_c$; the attenuation factor per unit length $m = \eta\omega l/c_g$, where c_g is the group speed of waves and $l = \pi L_x L_y/2(L_x + L_y)$ the mean free path; the dimensionless wavenumber $\kappa = kl/2\pi$, where $k = (\omega^2\, m/D)^{1/4}$ is the structural wavenumber. Such a representation is used to observe the diffuse field.

Figure 5 shows the evolution of diffuse field criterion for a single point force versus κ and η. The dotted line represents the modal overlap $M = 1$, the dashed line the attenuation factor $m = 2$ and the vertical solid line the number of modes $N = 10$. The presence of several points (A,B,C,D,E,F and G) is useful for the next paragraphs and sections.

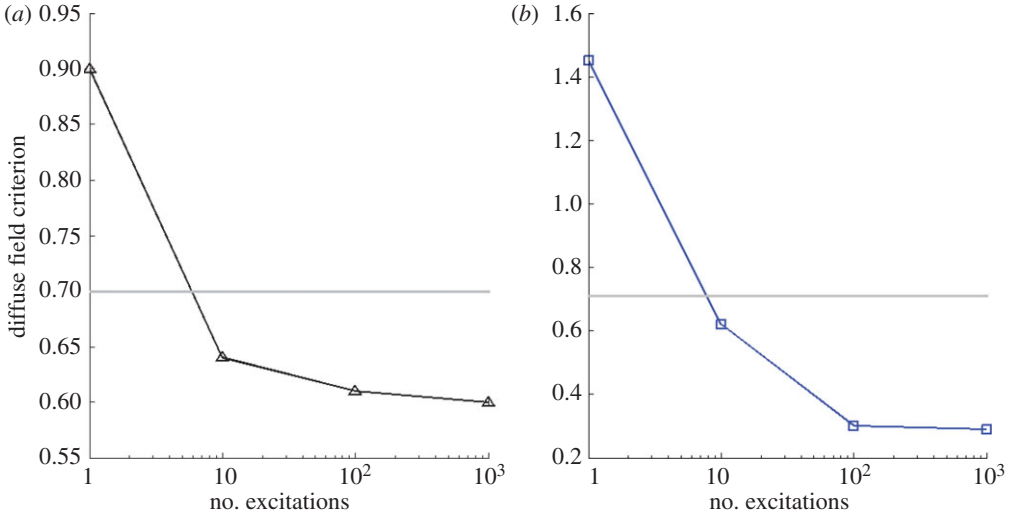

Figure 6. Evolution of the diffuse field criterion versus the number of uncorrelated random excitations. (*a*) From modal field to diffuse field ($\kappa = 1.29$, $f_c = 31.5$ Hz; $\eta = 0.03$); (*b*) from dominant direct field to diffuse field ($\kappa = 7.31$, $f_c = 1000$ Hz; $\eta = 0.1$). (Online version in colour.)

The $\sigma_d = 0.7$ contour line defines the area of a quasi-diffuse field. It occurs principally at high frequency and low damping. Above this contour line, increasing the damping, the criterion quickly increases showing a change in the energy field. The field is no more diffuse but is dominated by the direct field emanating from the point force. The 0.7 contour line is almost a straight line above $\kappa = 1.84$. As one can see, the dashed line representing the attenuation factor $m = 2$ fits well with that contour line. At low frequency (below $\kappa < 1.40$ or $N < 10$), the diffuse field criterion slightly increases. In these first frequency bands, only few modes are resonant and the energy field is dominated by a modal behaviour. The dotted line drawn in figure 5 shows values for which the modal overlap $M = 1$ occurs. It is often assumed that for energy methods such as SEA, the modal overlap of the structure has to be higher than one. This limit is clearly not correlated to the diffuse field criterion.

Figure 6 shows the evolution of the diffuse field criterion versus the number of point excitations with the same power spectral density. Two cases are tested represented by point A and point B in figure 5: in figure 6*a*, the field is modal with a single excitation ($\kappa = 1.29$, $f_c = 31.5$ Hz; $\eta = 0.03$; point A in figure 5). In figure 6*b*, the field is direct ($\kappa = 7.31$, $f_c = 1000$ Hz; $\eta = 0.1$) with a single excitation (point B in figure 5). In both cases, the criterion decreases going below 0.7 drawn in grey when the number of excitations increases (from 1 to 1000). A large number of excitations is a favourable condition for diffuse field. The fact that the criterion tends to non-zero limit may be explained by two approximations done in the simulation: first, the limited number of receiver points (3000) and the fact that the kinetic energy is arbitrary fixed at zero by the boundary conditions. By this second approximation, an outskirt area of the plate has a null energy density. The size of this area depends on wavelength and thus on the frequency band: the lower the frequency, the larger this area.

From figure 6, it is observed that even if a field is not diffuse for a single excitation ($\sigma_d > 0.7$), it becomes diffuse when a higher number of excitations is used. It means that if a field is not naturally diffuse in a subsystem (modal fields, direct fields) using a rain-on-the-roof excitation would enforce it to be diffuse. Consequently, the hypothesis of a rain-on-the-roof excitation implies the state of the diffuse field. The reciprocal is not verified because it has been shown that a field can be naturally diffuse even with a single excitation.

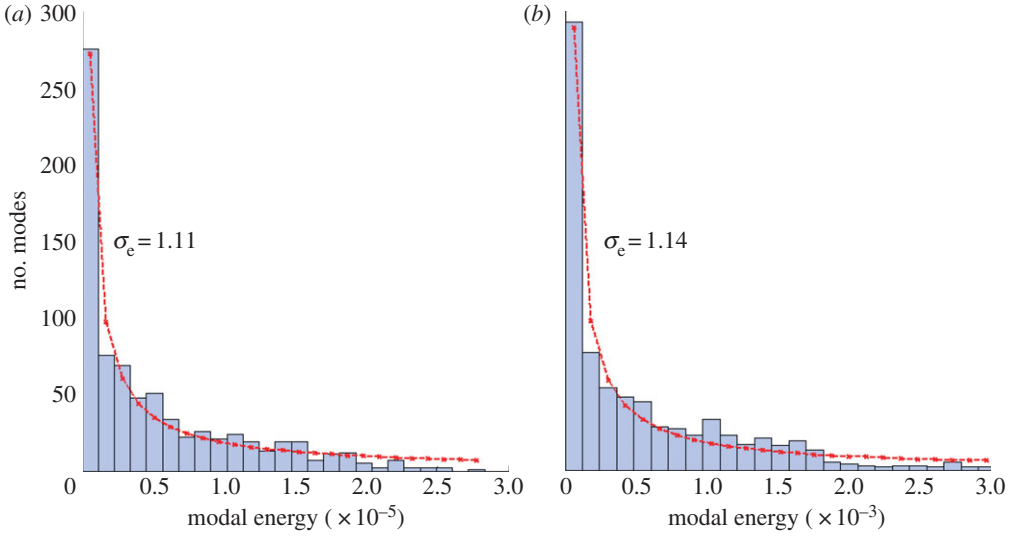

Figure 7. Repartition of modal energy for a rectangular plate excited by a single point force. (*a*) point C: ($\kappa = 14.63, f_c = 4$ kHz; $\eta = 0.1$) and (*b*) point D: ($\kappa = 14.63, f_c = 4$ kHz; $\eta = 0.001$). (Online version in colour.)

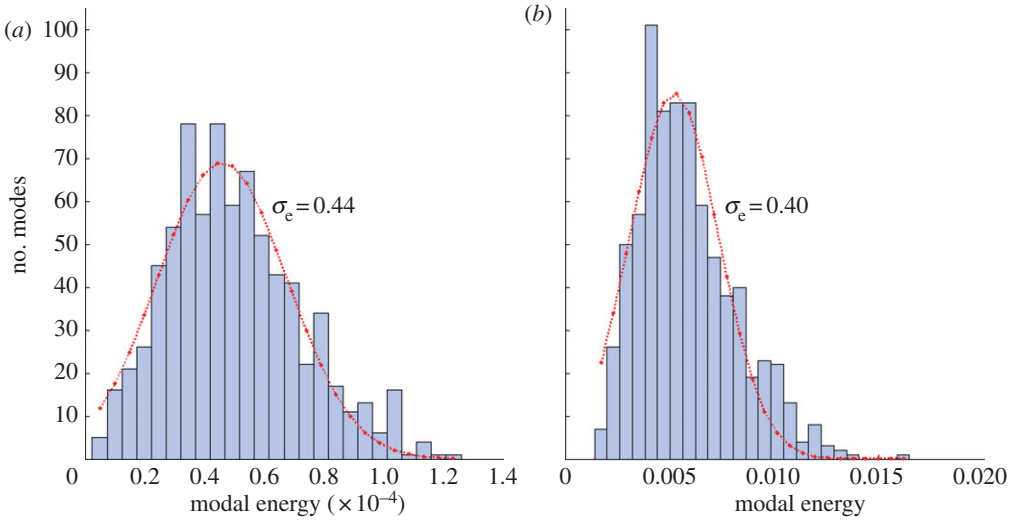

Figure 8. Repartition of modal energy repartition for a plate excited by 10 point forces. (*a*) Point C: ($\kappa = 14.63, f_c = 4$ kHz; $\eta = 0.1$) and (*b*) point D: ($\kappa = 14.63, f_c = 4$ kHz; $\eta = 0.001$). (Online version in colour.)

(ii) Energy equipartition

Figures 7 and 8 show the repartition of modal energy in two test cases: point C ($\kappa = 14.63$; $\eta = 0.1$) and point D ($\kappa = 14.63$; $\eta = 0.001$) from figure 5. The excitation is either a single (figure 7) or a group (figure 8) of random forces.

The repartition of the modal energy when the plate is excited by a single excitation is decreasing and can be fitted with a Weibull distribution. The first order of such a function reads

$$W(x, a, b) = abx^{b-1}\, e^{-ax^b}, \tag{4.13}$$

where a and b are adjustable parameters. About 36–38% of the total number of modes in the frequency band have a low modal energy value. Very few modes have the maximum of the modal energy ($\approx 0.3\%$). The equipartition criteria σ_e for each case are between 1.1 and 1.2. The frequency range influences the number of modes in the frequency band and the damping coefficient the value of modal energies, but the general distribution of modal energy is identical for both cases. In the simulation, $\eta = 0.1$ (figure 7*a*) gives ($a = 0.006$; $b = 0.063$) and $\eta = 0.001$ (figure 7*b*) gives ($a = 1.201$; $b = 0.049$). a and b have such values that the Weibull distribution can be approximated by,

$$W(x, a, b) \sim \frac{ab}{x}. \tag{4.14}$$

This clearly shows that equipartition is usually not fulfilled for a single excitation. Figure 8 shows the repartition of modal energy when 10 random excitations are used and for two cases of damping loss factor (point C—figure 8*a* and point D—figure 8*b*). These repartition can be fitted with Gaussian distributions

$$G(x, c, d, f) = c\mathrm{e}^{-((\mathrm{x}-d)/f)^2}, \tag{4.15}$$

where c, d and f are adjustable parameters. The case $\eta = 0.1$ gives ($c = 69.13$; $d = 4.584\mathrm{E}-5$; $f = 3.071\mathrm{E}-5$) and $\eta = 0.001$ gives ($c = 85.15$; $d = 5.207\mathrm{E}-3$; $f = 3.025\mathrm{E}-3$). The value of damping coefficient does not affect the repartition shape which is now centred on the mean value. The rain-on-the-roof excitation is therefore favourable for equipartition.

The results may be interpreted as follows. The general expression of the modal energy is in the special case of a single excitation,

$$\langle E_n \rangle(\omega_c) = \frac{S_0 \psi_n(x_i, y_i)^2}{2\pi} \int_{-\infty}^{+\infty} \omega^2 \frac{\mathrm{d}\omega}{m((\omega_n^2 - \omega^2)^2 + (\eta\omega_n\omega)^2} = \frac{S_0 \psi_n(x_i, y_i)^2}{2m\eta\omega_n}, \tag{4.16}$$

where the limit of integration of equation (4.10) have been extended to infinity for the sake of simplicity. The modal energy is therefore strongly dependent on the mode by the term ψ_n/ω_n which demonstrates that the energy is not equally distributed. On the contrary, for an infinite number of excitations and since $\lim_{N\to\infty}(1/N \sum_{i=1}^{N} \psi_n(x_i, y_i)^2) = 1/(L_x L_y)$. The expectation of the modal energy is

$$\langle E_n \rangle(\omega_c) = \sum_{i=1}^{N} \frac{S_0 \psi_n(x_i, y_i)^2}{2m\eta\omega_n} = \frac{NS_0}{L_x L_y 2m\eta\omega_n} \sim \frac{1}{\omega_n}. \tag{4.17}$$

The modal energy depends on the frequency. Consequently, a constant damping loss factor and a rain-on-the-roof excitation leads to a modal energy which is not equally distributed [27]. But when choosing another damping model, for example the one used by Lyon & Dejong [28] that is a half-power bandwidth $\Delta = \eta\omega_n$ constant then the modal energy becomes

$$\langle E_n \rangle(\omega_c) = \frac{NS_0}{L_x L_y m\Delta}. \tag{4.18}$$

In that case the energy is equally distributed between modes, the equipartition of modal energy is reached.

Figure 9 represents the repartition of modal energy for both models of damping. The centre frequency stays at $f_c = 4000\,\mathrm{Hz}$ and a group of 1000 random excitations is taken. The energy distribution is drawn in light grey when the modal damping ratio is maintained constant with $\eta = 0.01$ (diffuse field condition). It corresponds to a Gaussian distribution similar to the one in figure 8. Otherwise, when the half-power bandwidth defined as $\Delta = 4\pi\eta f_c = 502.65$ (in dark grey) is maintained constant the modal energy distribution is again a Gaussian but much tighter showing that the modal energies have closed values. The energy equipartition criterion is in that case three times lower ($\sigma_e = 0.067$ instead of $\sigma_e = 0.211$). This clearly shows that equipartition is reached when the modal forces have the same power spectral density (rain on the roof) and when the half-power bandwidth of modes is the same. The case of a coupled subsystem is discussed in [25]. For each of the damping models, two approximations are done: the truncation on the mode number and the number of excitation points which is finite.

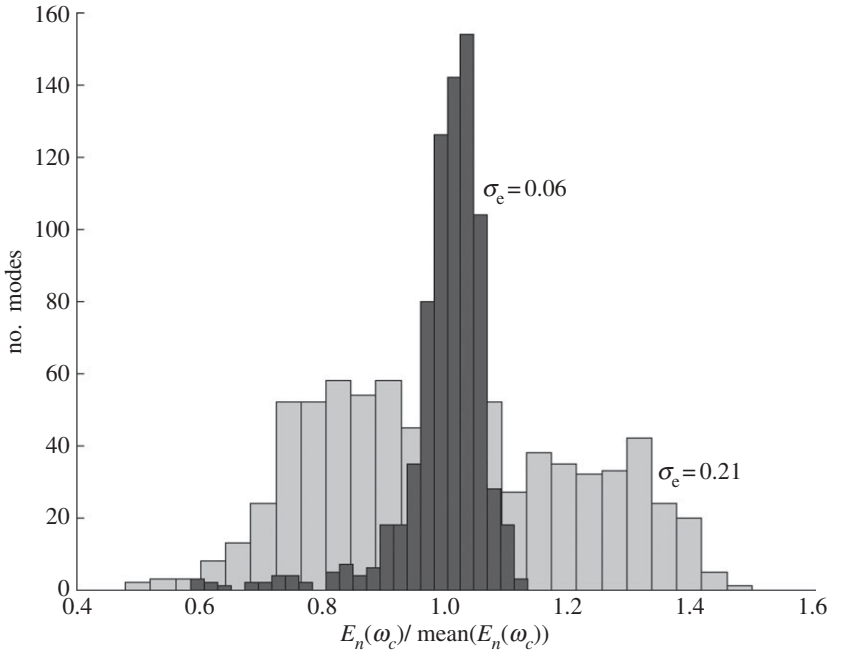

Figure 9. Modal energy repartition for a plate excited by 1000 random point forces. The centre frequency is $f_c = 4000$ Hz and the damping models are different: η constant ($\eta = 0.01$)—light grey and $\Delta = 4\pi\eta f_c$ constant ($\Delta = 502.65$)—dark grey repartition.

This simple simulation on a single plate highlights that energy equipartition is a direct consequence of rain-on-the-roof excitation, whereas the diffuse field state can be either reached by suitable values of damping and frequency or forced by a rain-on-the-roof excitation.

5. Case of two coupled subsystems

In this section, the expectation of local and modal energies in coupled plates are calculated to quantify the state of diffuse field and energy equipartition but also to evaluate the difference between SEA prediction and the reference calculation on the ratio of global energies. The case of two rectangular simply supported plates coupled by a spring is examined (figure 10).

(a) Assessment tools of the assumptions

w_A and w_B denote the deflection of plate A and plate B, K the coupling spring stiffness. If plate A is excited by a sum of stationary stochastic processes $f_i(x, y, t)$ which follows equation (4.2), the equations of motion are similar to equation (4.1) with an additional term for the coupling force,

$$D\nabla^4 w_A(x,y,t) + m\frac{\partial^2 w_A(x,y,t)}{\partial t^2} = f(x,y,t) + K(w_B(x_B,y_B,t) - w_A(x_A,y_A,t))\delta(x - x_A, y - y_A), \tag{5.1}$$

for plate A and

$$D\nabla^4 w_B(x,y,t) + m\frac{\partial^2 w_B(x,y,t)}{\partial t^2} = K(w_A(x_A,y_A,t) - w_B(x_B,y_B,t))\delta(x - x_B, y - y_B), \tag{5.2}$$

for plate B where x_A, y_A is the attached point of the spring on plate A and x_B, y_B on plate B.

Let $G^A(x, y; x_i, y_i, \omega)$ (resp. G^B) be the frequency response function of the coupled system for a receiver at x, y on plate A (resp. plate B) and a unit point force at x_i, y_i on plate A. To determine

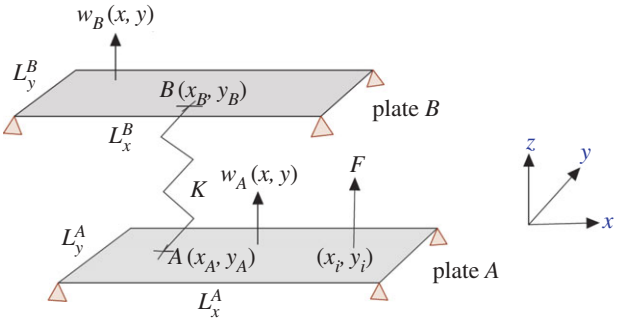

Figure 10. Simply supported plates coupled with stiffness K. Plate *A* is excited by a sum of random forces having the power spectral density of white noise. (Online version in colour.)

G^A, one introduces the frequency response functions of uncoupled plates

$$H^A(x, y; x_i, y_i, \omega) = \sum_{n\geq 0} \frac{\psi_n^A(x, y)\psi_n^A(x_i, y_i)}{m(\omega_{A,n}^2 - \omega^2 + j\eta_A\omega_{A,n}\omega)}, \tag{5.3}$$

where x_i, y_i may be either the position of an external force ($i = 1, 2..., N$) or the position of the coupling spring x_A, y_A and η_A, ψ^A denote respectively the damping coefficient and the mode shape of an isolated plate. The frequency response function for an isolated plate *B* is similar.

The deflections at any receiver point are given by

$$\left.\begin{aligned} G^A(x, y; x_i, y_i, \omega) &= H^A(x, y; x_i, y_i; \omega) + H^A(x, y; x_A, y_A; \omega)K[W^B(x_i, y_i; \omega) - W^A(x_i, y_i; \omega)], \\ \text{and} \quad G^B(x, y; x_B, y_B, \omega) &= H^B(x, y; x_B, y_B; \omega)K[W^A(x_i, y_i; \omega) - W^B(x_i, y_i; \omega)], \end{aligned}\right\} \tag{5.4}$$

where $W^A(x_i, y_i; \omega) = G^A(x_A, y_A; x_i, y_i, \omega)$ and $W^B(x_i, y_i; \omega) = G^B(x_B, y_B; x_i, y_i, \omega)$. The displacements W^A and W^B are found by substituting x, y with x_A, y_A and x_B, y_B,

$$\begin{bmatrix} 1 + KH^A(x_A, y_A; x_A, y_A; \omega) & -KH^A(x_A, y_A; x_A, y_A; \omega) \\ -KH^B(x_B, y_B; x_B, y_B; \omega) & 1 + KH^B(x_B, y_B; x_B, y_B; \omega) \end{bmatrix} \begin{bmatrix} W^A \\ W^B \end{bmatrix} = \begin{bmatrix} H^A(x_A, y_A; x_i, y_i; \omega) \\ 0 \end{bmatrix}. \tag{5.5}$$

Then, the frequency response function G^A and G^B at any receiver point are obtained by applying (5.4) with W^A and W^B just determined by equation (5.5).

(i) Local energy expectations

Using equation (4.7), the local energy density $\langle e\rangle(x, y, \omega_c)$ for plate *A* is given by

$$\langle e_A\rangle(x, y, \omega_c) = \sum_{i=1}^{N} \frac{S_i}{2\pi} m \int_{\Delta\omega} \omega^2 |G^A(x, y; x_i, y_i; \omega)|^2 \, \mathrm{d}\omega \tag{5.6}$$

idem for plate *B*.

(ii) Modal energy expectations

The expectations of the modal energies for the two plates are found using a similar development that was done for a single plate.

$$\langle E^A\rangle(\omega_c) = \int_{L_x^A} \int_{L_y^A} \langle e_A\rangle(x, y, \omega_c) \, \mathrm{d}x \, \mathrm{d}y \tag{5.7}$$

Table 2. General parameters of the coupled plates.

type	symbol	value	unit
plate A	$L_x^A \times L_y^A$	1.44×1.2	m^2
plate B	$L_x^B \times L_y^B$	1.39×1.1	m^2
density	ρ	7800	$kg\,m^{-3}$
Young's modulus	E	2.1E11	$N\,m^{-2}$
Poisson's ratio	ν	0.3	—
thickness	$h_A = h_B$	2	mm
coupling stiffness	K	981	$N\,m^{-1}$
mean free path	l_A	1.028	m
mean free path	l_B	0.964	m

idem for plate B. After calculation, the global energy of plate A is

$$\langle E^A\rangle(\omega_c) = \sum_{n\geq 0} \langle E_n^A\rangle(\omega_c), \tag{5.8}$$

where the modal energy expectation is

$$\langle E_n^A\rangle(\omega_c) = \sum_{i=1}^{N} \frac{S_i}{2\pi} \int_{\Delta\omega} \omega^2 \frac{|\psi_n^A(x_i,y_i) + K\psi_n^A(x_A,y_A)[W^B(x_i,y_i;\omega) - W^A(x_i,y_i;\omega)]|^2}{m((\omega_{A,n}^2 - \omega^2)^2 + (\eta_A\omega_{A,n}\omega)^2)}\,\mathrm{d}\omega, \tag{5.9}$$

for plate A and

$$\langle E_n^B\rangle(\omega_c) = \sum_{i=1}^{N} \frac{S_i}{2\pi} \int_{\Delta\omega} \omega^2 \frac{|K\psi_n^B(x_B,y_B)[W^A((x_i,y_i;\omega)) - W^B((x_i,y_i;\omega))]|^2}{m((\omega_{B,n}^2 - \omega^2)^2 + (\eta_B\omega_{B,n}\omega)^2)}\,\mathrm{d}\omega, \tag{5.10}$$

for plate B.

(b) Discussion on the assumptions

The parameters used for the numerical simulation are presented in table 2. The computation of the expectations of local and modal energies follow the equations (5.6), (5.9) and (5.10). A various number of random excitations is applied on plate A (from 1 to 100) with a uniform distribution. There are 3000 receivers points which are randomly and uniformly placed on both plates. The coupling spring is attached with plate A at $x_A = 0.72, y_A = 0.6$ and with plate B at $x_B = 0.38, y_B = 1.06$. The energy equipartition and diffuse field criteria are computed on each octave band. Moreover, similarly with the case of a single plate, only resonant modes within the frequency band are taken in the calculation of H^A and H^B.

The evolution of the diffuse field and the equipartition criteria for both plates are carried out at high frequency ($f_c = 2000$ Hz) and high damping ($\eta_A = \eta_B = 0.1$) (point E from figure 5) in figure 11 while the number of random excitation increases. Concerning the diffuse state (figure 11*a*), results for coupled plates are along the lines of what has been said for a single plate. When plate A is excited by a single point force the diffuse field criterion is high ($\sigma_d \approx 2.8$) indicating a strongly non-diffuse state. The energy is transferred to plate B via the stiffness which acts as a located point force. The diffuse field criterion of plate B has consequently a high value ($\sigma_d \approx 2.8$), and the field in plate B is strongly non-diffuse. When the number of excitations increases up to one hundred the diffuse field criterion of plate A decreases showing that the field becomes diffuse in plate A. But the diffuse field criterion stays high for plate B, because the excitation remains a single point force. The dispersion bars are computed for a population of 10 simulations. They are large with few excitations, because results are strongly dependent on the excitation and receiver positions.

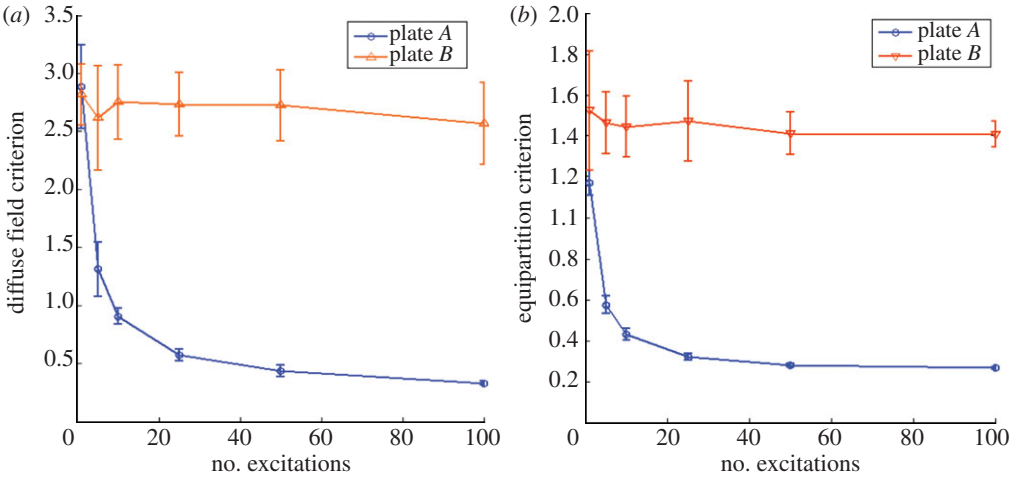

Figure 11. (*a*,*b*) Diffuse field and energy equipartition criteria evolution versus number of excitations for two coupled plates at point E: ($\kappa = 10.35$, $f_c = 2$ kHz; $\eta_A = \eta_B = 0.1$). (Online version in colour.)

For the energy equipartition criterion (figure 11*b*), results are again in agreement with those of an isolated plate: a decrease of the criterion for plate *A* is observed meaning that rain-on-the-roof excitation is favourable to equipartition. The dispersion bars are high for both plates with few excitations and quickly decrease. The energy equipartition criterion for plate *B* stays high ($\sigma_e \approx 1.17$) because it is still excited by a single source. The modal energy distribution is never equally distributed in plate *B*.

(c) Evaluation of the coupling power proportionality

The global energies ratio given by equation (5.8) are now compared with their SEA predictions.

(i) Statistical energy analysis approach

For two coupled subsystems *A* and *B*, where *A* is excited by a force field supplying a mean power $\langle P_A \rangle$, the energy balance of each subsystem jointly with the coupling power proportionality leads to the standard SEA equation [28],

$$\frac{1}{\omega_c}\begin{pmatrix}\langle P_A\rangle \\ 0\end{pmatrix} = \begin{bmatrix}\eta_A + \eta_{AB} & -\eta_{BA} \\ -\eta_{AB} & \eta_B + \eta_{BA}\end{bmatrix}\begin{bmatrix}\langle E^A\rangle \\ \langle E^B\rangle\end{bmatrix}, \tag{5.11}$$

where η_A, η_B are the internal damping of subsystems *A* and *B*. The coupling loss factors η_{AB} and η_{BA} for two plates coupled by a spring are given by Mace & Li [27]

$$\omega_c n_A \eta_{AB} = \omega_c n_B \eta_{BA} = \frac{K^2}{32\pi\omega^2}\frac{1}{\sqrt{\rho_A h_A D_A}\sqrt{\rho_B h_B D_B}}, \tag{5.12}$$

where D_A, D_B are the bending stiffness of plate *A* and *B* and n_A, $n_B = L_x L_y \sqrt{m/D}/(4\pi)$ are the modal densities. The energy ratio predicted by SEA is therefore

$$\left(\frac{\langle E^B\rangle}{\langle E^A\rangle}\right)_{\mathrm{SEA}} = \frac{n_B/n_A}{1 + \eta_B/\eta_{BA}}. \tag{5.13}$$

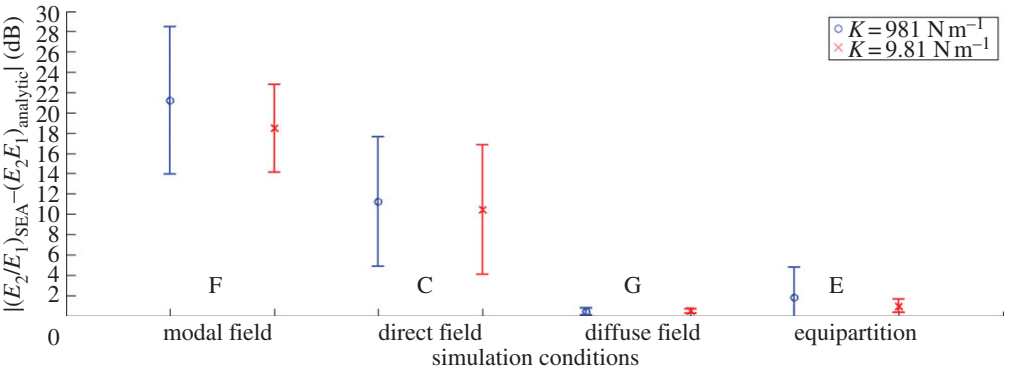

Figure 12. Error between SEA and the reference method for several conditions: modal field—point F: ($\kappa = 1.29$; $\eta_A = \eta_B = 0.001$) 1 excitation; direct field—point C: ($\kappa = 14.35$; $\eta_A = \eta_B = 0.1$) 1 excitation; diffuse field—point G: ($\kappa = 29.27$, $f_c = 16$ kHz; $\eta_A = \eta_B = 0.0001$) 1 excitation; energy equipartition—point E: ($\kappa = 10.35$; $\eta_A = \eta_B = 0.1$) 100 excitations. (Online version in colour.)

(ii) Difference between statistical energy analysis and reference

The error of SEA compared with the governing equations is

$$\Delta_{\text{SEA-reference}} = \left| 10\log\left(\frac{\langle E^B\rangle}{\langle E^A\rangle}\right)_{\text{SEA}} - 10\log\left(\frac{\langle E^B\rangle}{\langle E^A\rangle}\right)_{\text{reference}} \right|, \tag{5.14}$$

where $\langle E^B\rangle/\langle E^A\rangle_{\text{SEA}}$ is estimated by equation (5.13) and the reference ratio by equation (5.8).

Figure 12 illustrates the error $\Delta_{\text{SEA-reference}}$ for different conditions of simulations (repeated 10 times to compute the dispersion as excitations are randomly distributed). The coupling stiffness varies for each simulation ($K = 981\ \text{N m}^{-1}$ circle marker or $K = 9.81\ \text{N m}^{-1}$ cross marker). The conditions of modal field on plate A corresponds to point F in figure 5 ($f_c = 31.5$ Hz, $\kappa = 1.29$; $\eta_A = \eta_B = 0.001$) with a single point force. The error is important whatever the coupling strength is (around 20 dB with a coupling of $K = 981\ \text{N m}^{-1}$) with a large dispersion. The criteria of diffuse field and energy equipartition are $\sigma_d^A = 0.75$, $\sigma_d^B = 0.97$, $\sigma_e^A = 0.88$ and $\sigma_e^B = 1.23$ showing that these assumptions are not fulfilled. On the modal field domain where there is neither diffuse field nor energy equipartition SEA tends to overestimate the energy transfers.

Direct field conditions are set up with a large damping coefficient ($\eta_A = \eta_B = 0.1$) a high frequency ($f_c = 4$ kHz, $\kappa = 14.35$) and a single excitation (point C in figure 5). The error is still high (≈ 11 dB) as well as dispersion. The criteria show that the conditions of equipartition and diffuse field are not respected ($\sigma_d^A = 3.03$, $\sigma_d^B = 3.56$, $\sigma_e^A = 1.20$ and $\sigma_e^B = 2.39$) which confirms that SEA cannot be used in such a case.

Plate A is in diffuse field condition ($\sigma_d^A = 0.12$ and $\sigma_d^B = 0.19$) when the damping is low, the excitation is single and the frequency band is high (point G). In that case, the difference between SEA and reference is near zero which means that a diffuse field state is a sufficient condition for SEA even if neither the hypothesis of rain-on-the-roof nor energy equipartition are fulfilled.

Finally, being in an energy equipartition condition (100 excitations, $\eta_A = \eta_B = 0.1$, $f_c = 2$ kHz, $\kappa = 10.35$ represented by point E) permits to apply correctly SEA. The energy equipartition criteria are in that case $\sigma_e^A = 0.25$ and $\sigma_e^B = 1.30$. The measured error ranges from 1 to 2 dB which may be improved with a lighter coupling stiffness.

6. Conclusion

It has been shown that a rain-on-the-roof excitation usually implies a diffuse field state whatever the damping and the frequency band. Contrarily, a point force can produce a diffuse field if

the damping is low and the frequency is high. The case of two coupled plates confirms these observations made for a single plate.

The vibrational energy is equally distributed among modes when a rain-on-the-roof excitation is applied provided that the half-power bandwidth is maintained constant. But, in the meantime, the field becomes diffuse. This observation is valid for all studied frequency/damping cases. Consequently, energy equipartition indirectly implies a diffuse field.

The two test cases reveal that the assumption with the larger domain of validity is the diffuse field assumption (it consists of the domain of validity of the other assumptions plus the case of a point force under low damping and high frequency). However, one must remember that diffuse field and equipartition are consequences of the type of excitation and the internal properties of the structure (either single excitation in the diffuse field domain or rain-on-the-roof excitation). Assuming diffuse field or energy equipartition allows the use of SEA but is complicated to check based on theory. This is why to be sure that SEA may be applied, it is more convenient to assume rain-on-the-roof excitation.

Acknowledgements. This work was supported by the Labex CeLyA of Universite de Lyon, operated by the French National Research Agency (ANR-10-LABX-0060/ANR-11-IDEX-0007).

References

1. Lyon RH, Maidanik G. 1962 Power flow between linearly coupled oscillators. *J. Acoust. Soc. Am.* **34**, 623–639. (doi:10.1121/1.1918177)
2. Lyon RH, Eichler E. 1964 Random vibration of connected structures. *J. Acoust. Soc. Am.* **36**, 1344–1354. (doi:10.1121/1.1919207)
3. Lyon RH, Scharton TD. 1965 Vibrational-energy transmission in a three-element structure. *J. Acoust. Soc. Am.* **38**, 253–261. (doi:10.1121/1.1909649)
4. Le Bot A, Carcaterra A, Mazuyer D. 2010 Statistical vibroacoustics and entropy concept. *Entropy* **12**, 2418–2435. (doi:10.3390/e12122418)
5. Mace B. 1994 On the statistical energy analysis hypothesis of coupling power proportionality and some implications of its failure. *J. Sound Vib.* **178**, 95–112. (doi:10.1006/jsvi.1994.1470)
6. Fahy F. 1994 Statistical energy analysis: a critical overview. *Phil. Trans. R. Soc. Lond. A* **346**, 431–447. (doi:10.1098/rsta.1994.0027)
7. Crandall SH, Lotz R. 1971 On the coupling loss factor in statistical energy analysis. *J. Acoust. Soc. Am.* **49**, 352–356. (doi:10.1121/1.1912337)
8. Langley RS, Heron KH. 1990 Elastic wave transmission through plate/beam junctions. *J. Sound Vib.* **143**, 241–253. (doi:10.1016/0022-460X(90)90953-W)
9. Wohle W, Beckmann TH, Schreckenbach H. 1981 Coupling loss factors for statistical energy analysis of sound transmission at rectangular structural slab joints. I. *J. Sound Vib.* **77**, 323–334. (doi:10.1016/S0022-460X(81)80169-1)
10. Wohle W, Beckmann TH, Schreckenbach H. 1981 Coupling loss factors for statistical energy analysis of sound transmission at rectangular structural slab joints. II. *J. Sound Vib.* **77**, 335–344. (doi:10.1016/S0022-460X(81)80170-8)
11. Keane AJ, Prince WG. 1987 Statistical energy analysis of strongly coupled systems. *J. Sound Vib.* **117**, 363–386. (doi:10.1016/0022-460X(87)90545-1)
12. Kishimoto Y, Berrnstein DS. 1995 Thermodynamic modelling of interconnected systems, part I Conservative coupling. *J. Sound Vib.* **182**, 23–58. (doi:10.1006/jsvi.1995.0181)
13. Fahy F, De Yuan Y. 1987 Power flow between non-conservatively coupled oscillators. *J. Sound Vib.* **114**, 1–11. (doi:10.1016/S0022-460X(87)80227-4)
14. Sun JC, Lalor N, Richards EJ. 1987 Power flow and energy balance of non-conservatively coupled structures, I: theory. *J. Sound Vib.* **112**, 321–330. (doi:10.1016/S0022-460X(87)80199-2)
15. Mace B. 2003 Statistical energy analysis, energy distribution models and system modes. *J. Sound Vib.* **264**, 391–409. (doi:10.1016/S0022-460X(02)01201-4)
16. Maxit L, Guyader J-L. 2003 Extension of SEA model to subsystems with non-uniform modal energy distribution. *J. Sound Vib.* **265**, 337–358. (doi:10.1016/S0022-460X(02)01459-1)
17. Totaro N, Guyader J-L. 2012 Extension of statistical modal energy distribution analysis for estimating energy density in coupled subsystem. *J. Sound Vib.* **331**, 3114–3129. (doi:10.1016/j.jsv.2012.02.015)

18. Totaro N, Guyader J-L. 2013 Modal energy analysis. *J. Sound Vib.* **332**, 3735–3749. (doi:10.1016/j.jsv.2013.02.022)
19. Langley RS. 1992 A wave intensity technique for the analysis of high frequency vibrations. *J. Sound Vib.* **159**, 483–502. (doi:10.1016/0022-460X(92)90754-L)
20. Le Bot A. 1998 A vibroacoustic model for high frequency analysis. *J. Sound Vib.* **211**, 537–554. (doi:10.1006/jsvi.1997.1378)
21. Le Bot A. 2002 Energy transfer for high frequencies in build-up structures. *J. Sound Vib.* **250**, 247–275. (doi:10.1006/jsvi.2001.3933)
22. Scharton TD, Lyon RH. 1968 Power flow and energy sharing in random vibration. *J. Acoust. Soc. Am.* **43**, 1332–1343. (doi:10.1121/1.1910990)
23. Newland DE. 1966 Power flow between a class of coupled oscillators. *J. Acoust. Soc. Am.* **43**, 553–559. (doi:10.1121/1.1910865)
24. Finnveden S. 2011 A quantitative criterion validating coupling power proportionality in statistical energy analysis. *J. Sound Vib.* **330**, 89–109. (doi:10.1016/j.jsv.2010.08.003)
25. Ungar EE. 1966 *Fundamentals of statistical energy analysis of vibrating systems*. Technical report AFFDL-TR-66-52. Cambridge, MA: Bolt Beranek and Newman Inc.
26. Newland DE. 1968 Power flow between a class of coupled oscillators. *J. Acoust. Soc. Am.* **43**, 553–559. (doi:10.1121/1.1910865)
27. Mace B, Li J. 2007 The statistical energy analysis of coupled sets of oscillators. *Proc. R. Soc. A.* **463**, 1359–1377. (doi:10.1098/rspa.2007.1824)
28. Lyon RH, Dejong R. 1995 *Theory and application of statistical energy analysis*. Boston, MA: Butterworth-Heinemann.
29. Lesueur C. 1988 *Rayonnement acoustique des structures*. Paris, France: Eyrolles.
30. Lyon RH. 1973 *Methodes d'analyse statistique de l'energie*. Lectures given by R.H. Lyon on 16–18 January 1973 at the Ecole centrale de Lyon, Ecully, France.
31. Lotz R, Crandall SH. 1973 Prediction and measurement of the proportionality constant in statistical energy analysis. *J. Acoust. Soc. Am.* **54**, 516–524. (doi:10.1121/1.1913609)
32. Maxit L, Guyader J-L. 2001 Estimation of SEA coupling loss factors using a dual formulation and FEM modal information, part I: theory. *J. Sound Vib.* **239**, 907–930. (doi:10.1006/jsvi.2000.3192)
33. Maxit L, Guyader J-L. 2001 Estimation of SEA coupling loss factors using a dual formulation and FEM modal information, part II: numerical applications. *J. Sound Vib.* **239**, 931–948. (doi:10.1006/jsvi.2000.3193)
34. Totaro N. 2009 SEA coupling loss factors of complex vibro-acoustic systems. *J. Vib. Acoust.* **131**, 410 091–410 098. (doi:10.1115/1.3086929)
35. Maidanik G, Dickey J. 1990 Wave derivation of the energetics of driven coupled one-dimensional dynamic systems. *J. Sound Vib.* **139**, 31–42. (doi:10.1016/0022-460X(90)90773-S)
36. Le Bot A. 2007 Derivation of statistical energy analysis from radiative exchanges *J. Sound Vib.* **300**, 763–779. (doi:10.1016/j.jsv.2006.08.033)
37. Lyon RH. 2003 Fluctuation theory and (very) early statistical energy analysis. *J. Acoust. Soc. Am.* **113**, 2401–2403. (doi:10.1121/1.1567274)
38. Kishimoto Y, Berrnstein DS. 1995 Thermodynamic modelling of interconnected systems, part II. Dissipative coupling. *J. Sound Vib.* **182**, 23–58. (doi:10.1006/jsvi.1995.0181)
39. Hassad WM, Chellaboina V, Nersesov SG. 2005 *Thermodynamics*. Princeton Series in Applied Mathematics. Princeton, NJ: Princeton University Press.
40. Carcaterra A. 2005 Ensemble energy average and energy flow relationships for nonstationary vibrating systems. *J. Sound Vib.* **288**, 751–790. (doi:10.1016/j.jsv.2005.07.015)
41. Carcaterra A. 2002 An entropy formulation for the analysis of energy flow between mechanical resonators. *Mech. Syst. Signal Process.* **16**, 905–920. (doi:10.1006/mssp.2002.1486)
42. Le Bot A. 2009 Entropy in statistical energy analysis. *J. Acoust. Soc. Am.* **125**, 1473–1478. (doi:10.1121/1.3075613)
43. Langley RS, Shorter PJ. 2002 Diffuse wavefields in cylindrical coordinates. *J. Acoust. Soc. Am.* **112**, 1465–1470. (doi:10.1121/1.1502895)
44. Rossi M. 2007 *Audio*. Lausanne, Switzerland: Presses Polytechniques et Universitaires Romandes.
45. Faller C. 2010 *Signal processing for audio and acoustics*. Lausanne, Switzerland: EPFL.
46. Lyon R. 1974 A new definition of diffusion. *J. Acoust. Soc. Am.* **56**, 1300–1302. (doi:10.1121/1.1903425)

47. Fahy FJ. 1985 *Sound and structural vibration*. London, UK: Academic Press.
48. Weaver RL. 2001 Equipartition and mean-square response in large undamped structure. *J. Acoust. Soc. Am.* **110**, 894–903. (doi:10.1121/1.1385566)
49. Roveri N, Carcaterra A. 2009 Energy equipartition and frequency distribution in complex attachments. *J. Acoust. Soc. Am.* **126**, 122–128. (doi:10.1121/1.3147502)
50. Magionesi F, Carcaterra A. 2009 Insights into energy equipartition principle in large undamped structures. *J. Sound Vib.* **322**, 851–869. (doi:10.1016/j.jsv.2008.11.038)
51. Fahy F. 1970 Energy flow between oscillators: special case of point excitation. *J. Sound Vib.* **11**, 481–483. (doi:10.1016/S0022-460X(70)80012-8)
52. Soedel W. 2004 *Vibrations of shells and plates*. New York, NY: Marcel Dekker.
53. Guyader J-L. 2002 *Vibrations in continuous media*. Paris, France: ISTE.
54. Le Bot A, Cotoni V. 2010 Validity diagrams of statistical energy analysis. *J. Sound Vib.* **329**, 221–235. (doi:10.1016/j.jsv.2009.09.008)